BUILDING ATTRIBUTES ACQUISITION USING HIGH RESOLUTION SATELLITE SAR DATA AND AIRBORNE LIDAR DATA

Tatsuya Yamamoto, Masafumi Nakagawa

Department of Civil Engineering, Shibaura Institute of Technology

h10082@shibaura-it.ac.jp

ABSTRACT

A frequent map revision is required in GIS applications, such as disaster prevention and urban planning. In general, airborne photogrammetry and LiDAR measurements are applied to geometrical data acquisition for automated map generation and revision. However, ground surveys and manual editing works are finally required for attribute data classification. On the other hand, SAR data enable automation of attribute data acquisition and classification. The SAR data represent microwave reflections on various ground surfaces and buildings. In our experiment, we extracted 1778 building roof segments from the digital surface model (DSM). In the classification step, we classified normalized radar cross-section (NRCS) values of ascending and descending orbit data into several clusters based on ISODATA clustering to estimate building attributes. We conducted an experiment to validate our approach and clarified that a combination of airborne LiDAR and satellite SAR data could extract and classify buildings in a dense urban area.

1. INTRODUCTION

A frequent map revision is required in GIS applications, such as disaster prevention and urban planning. In general, airborne photogrammetry and LiDAR measurements are applied to geometrical data acquisition for automated map generation and revision. In airborne photogrammetry, geometrical modeling and object classification can be automated using color images. Stereo matching is an essential technique for reconstructing a three-dimensional (3D) model from images. Recently, structure-from-motion (SfM) was applied to 3D modeling using random images (Uchiyama, 2014). Although object classification methods can be automated using height data estimated with stereo matching and SfM, construction materials such as wood and concrete are not easy to recognize. Construction materials constitute significant attribute data in building modeling and mapping. Therefore, ground surveys and manual editing works are required for attribute data classification.

In LiDAR measurements, modeling and object classification are also automated by point cloud segmentation (Sithole, 2003). The data intensity assists in object classification (Antonarakis, 2008). Moreover, data fusion approaches using aerial images and LiDAR data are also applied to object classification to improve modeling accuracy and processing times (Uemura, 2011).

On the other hand, although geometrical data extraction is not easy, SAR data enable automation of attribute data acquisition and classification. The SAR data represent microwave reflections on various ground surfaces and buildings. There are many studies related to monitoring activities of disaster, vegetation, and urban. Moreover, recent sensors, such as ALOS-2 PALSAR-2 (Japan Aerospace Exploration Agency, 2014), can acquire higher resolution data in urban areas. Therefore, we focused on the integration of airborne LiDAR data and high-resolution satellite SAR data for building extraction and classification.

2. METHODOLOGY

Our process is shown in Figure 1.

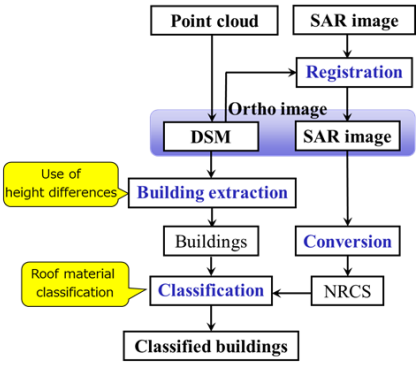

Fig. 1 Our process flow

First, we generated a digital surface model (DSM) from airborne LiDAR data. Second, the SAR image was registered with the DSM. Third, a normalized radar cross-section (NRCS) image was generated from SAR data. Fourth, building footprints were extracted from the DSM using height difference. Finally, building roof materials were classified with NRCS values in the DSM.

2.1 Building Footprint Extraction

Building footprints were extracted from the DSM in four steps (Fig. 2).

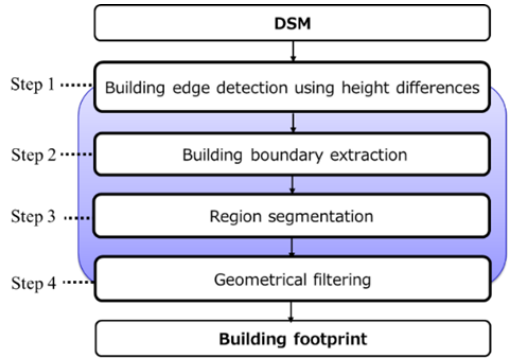

Fig. 2 Process flow of building footprint extraction

First, building edges were detected using height differences between the building roofs and ground surfaces from the DSM with a 3 times 3 operator. Even when the building edges were discontinuous, approximate building features were detected in this step. Second, building boundaries were extracted. Discontinuous edges were connected to each other in the DSM with 8-neighborhood pixel filtering. The connected edges were defined as building boundaries. Third, segmentation was applied to each region enclosed by the building boundary to refine the building's footprint. Although the extracted region included numerous noises, such as bridges, street trees, and automobiles, an approximate geometry of each region was extracted in this step. Finally, each region segment was filtered with its perimeter and area to extract the building's footprint. An example of the building extraction is shown in Figure 3.

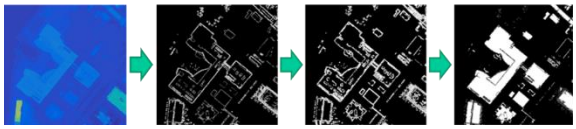

Fig. 3 Example of building extraction

2.2 Building Classification

Buildings were classified into several groups with nonsupervised classification. Our approach was a building classification based on roof materials with NRCS values. In this study, ISODATA clustering algorithm was applied to the building classification. In general, SAR data processing has several technical issues, such as layover, radar shadow, and foreshortening. These issues are caused by undulating grounds. Therefore, we focused on the use of a descending and ascending dataset to improve these issues.

3. EXPERIMENT

3.1 Study Area

We selected the Toyosu area in Tokyo as our study area. This area included various types of buildings, such as residential houses, high-rise buildings, and shopping malls (Fig.4).

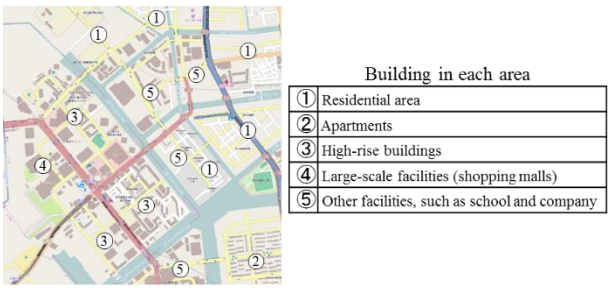

Fig. 4 Study area

3.2 Data Specification

We prepared point cloud data acquired with airborne LiDAR data and satellite SAR data (Figure 5 and Figure 6). The specifications of these data are shown in Tables 1 and 2. Table 3 shows the threshold values used for building extraction.

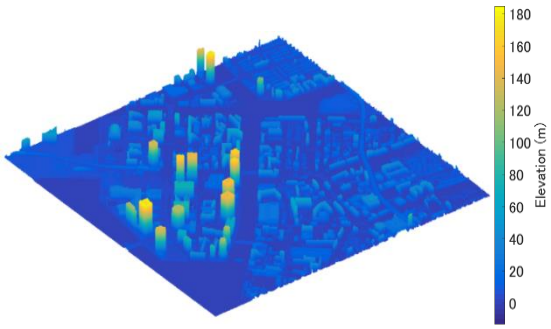

Fig. 5 Experiment data (Airborne LiDAR)

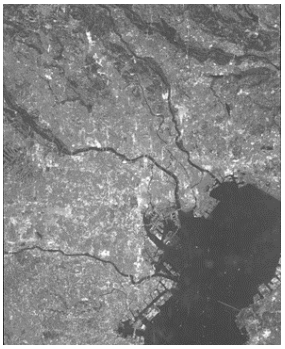

Fig. 6 Experiment data (SAR data)

Table 1. Specification of LiDAR data

Observer	Date	Spatial resolution	Data size
Aero Asahi Co., Ltd	26, October, 2013	0.1m~0.5m	Point cloud: 23,000,141 points

Table 2. Specification of PALSAR-2 data

Observer	Date	Spatial resolution	Polarized wave	Orbit
JAXA	14, February 2015	2.5m	HH	Descending
	13, February 2015	2.5m	HH	Ascending

Table 3. Threshold values

	Step 1	Step 2	Step 2	Step 4
Height	2 m	±0.2 m	1.5 m	---
Area	---	---	---	200 pixels
Perimeter	---	---	---	8000 pixels

3.3 Registration

The registration between SAR and LiDAR data required corresponding points to be extracted from each datum. Although SAR and LiDAR data had different indices, feature points could be selected manually, such as road intersections, rivers, and bridges. An example of corresponding points between SAR and LiDAR data is shown in Figure 7.

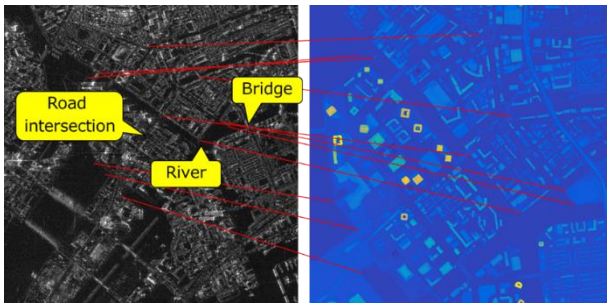

Fig. 7 Example of corresponded points

After the feature extraction procedure, the digital number (DN) of the SAR image was converted into an orthoimage of NRCS. We used the following transformation formula with the calibration factor (CF). We substituted –83 for the CF (ALOS-2 / Calibration Result of JAXA standard products, 2015).

$$NRCS(dB) = 10 \times log10(DN2) + CF \quad (1)$$

We selected several corresponding points, such as road intersections, rivers, and bridges, from each orthoimage. Moreover, an affine transformation was applied to the image registration between the SAR and LiDAR data.

4. RESULTS

4.1 Building Extraction

White regions indicate extracted building footprints. Figure 8 shows the result of Step 4.

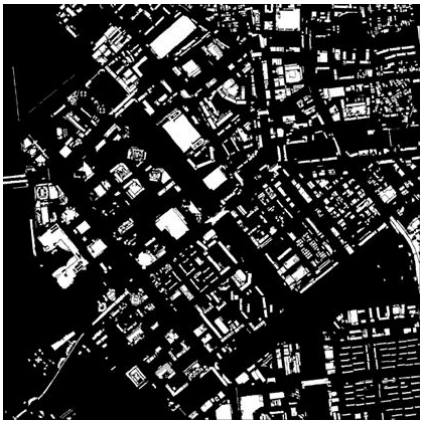

Fig. 8 Result of building extraction result

4.2 Building Classification

First, we extracted 1778 buildings from the DSM. Next, buildings were classified 10 clusters with nonsupervised classification. The result after the building classification based on ISODATA clustering of NRCS values is shown in Figure 9. The vertical axis indicates NRCS values calculated from ascending data, and the horizontal axis from descending data. Classified buildings with NRCS values were projected into an orthoimage (Fig. 10).

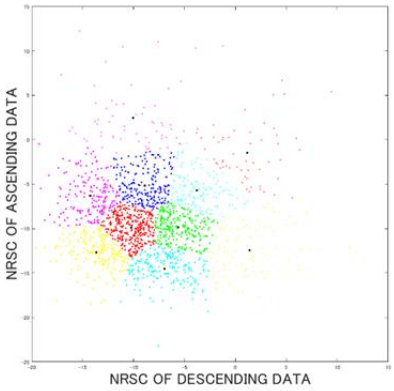

Fig. 9 ISODATA clustering result

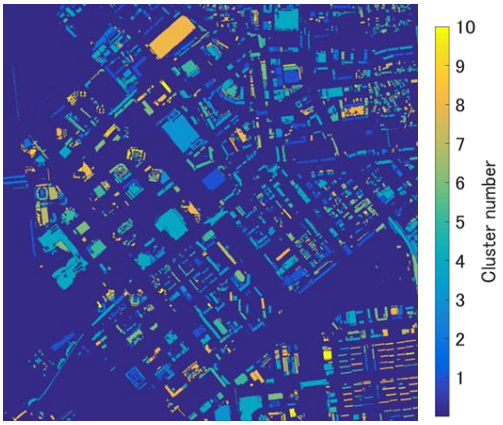

Fig. 10 Building classification result

5. DISCUSSION

In this study, although we focused on NRCS values of building roofs, we reviewed that more geometrical clues from aerial LiDAR data were more efficient for attribute data estimation. Slope parameter estimation from LiDAR data (Susaki, 2012) is one of the approaches for providing these geometrical clues. We expected that vector data extraction based on active contour models (Kass, 1987) could provide the geometrical clues from the DSM. Moreover, we also expect that vector data extraction based on a wall surface estimation using point cloud (Figure 11) could find borderlines of overcrowded buildings to improve our classification accuracy.

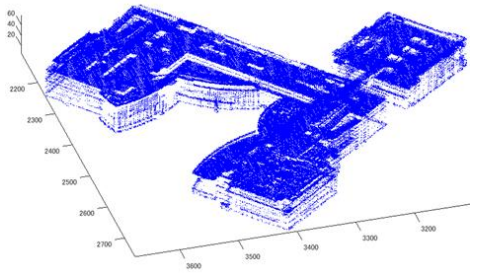

Fig. 11 Visualized building from vector data

In our experiment, although visual checks were required for determining the adequate threshold values, buildings were extracted from the DSM with our object extraction procedure. However, several small noises, such as automobiles, were left as unknown objects in the DSM. We expect that a semantic approach using road connections could improve our feature extraction accuracy. Additionally, although shadow detection is required, we expect that a combination of LiDAR data with aerial images could improve our building extraction accuracy.

In general, SAR data have several technical issues, such as layover, radar shadow, and foreshortening. However, we confirmed that dense point cloud data could recognize ground surfaces to avoid these issues automatically. Moreover, 3D geometrical data generated from the point cloud could be used for cardinal effect estimation.

6. CONCLUSION

In this paper, we focused on the integration of LiDAR and SAR data to achieve frequent map updates with attribute data acquisition. First, we generated a DSM from a point cloud acquired with airborne LiDAR. Second, the DSM was registered with the SAR data to overlay NRCS values. Third, buildings were extracted from the DSM. Finally, we classified buildings into several clusters.

In our experiment, we prepared point cloud data acquired with an airborne LiDAR and satellite SAR data acquired with ALOS-2 PALSAR-2 in Tokyo. Next, we extracted 1778 buildings in a DSM generated from the LiDAR data. Although our result included noises such as bridges and automobiles, we classified buildings into ten clusters with NRCS values. In this study, we showed that a combination of airborne LiDAR and satellite SAR data could extract and classify buildings in an urban dense area. In our future works, we will apply the supervised clustering with a semantic approach to improve classification accuracy.

REFERENCES

Antonarakis, A, S., Richards, K, S., Brasington, J., Remote Sensing of Environment, Volume 112, Issue 6, pp. 2988-2998, 2008.

ALOS-2/ALOS@EORC Homepage, ALOS-2 / Calibration Result of JAXA standard products, 2014. Retrieved 21 July 2015, from http://www.eorc.jaxa.jp/en/about/distribution/info/alos/20090109en_3.html.

Japan Aerospace Exploration Agency, Advanced Observing Satellite-2 “DAICHI-2” (ALOS-2). Retrieved 27 July 2013, from http://global.jaxa.jp/projects/sat/alos2/

Kass,M., Witkin, A., Terzopoulos, D., International Journal of Computer Vision, pp. 321-331, 1988.

Sithole, G., Vosselman, G., Remote Sensing and Data Fusion over Urban Areas. 2nd GRSS/ISPRS Joint Workshop on, pp. 67-71, 2003.

Susaki, J., Remote Sensing 2012, Volume 4, Issue 6, pp. 1804-1819, 2012.

Uchiyama, S., Inoue, H., Suzuki, H., Report of the National Research Institute for Earth Science and Disaster Prevention, Volume 81, pp. 37-60, 2014.

Uemura, T., Uchimura, K., koutaki, G., Journal of The Institute of Image Electronics Engineers of Japan, Volume 40, No.1, pp. 74-85, 2011.

ACKNOWLEDGMENT

This work is supported by Japan Aerospace Exploration Agency. Moreover, our experiments are supported by Aero Asahi Co. Ltd.